Supporting Information

Low-cost and High-power $K_4[Mn_2Fe](PO_4)_2(P_2O_7)$ as a novel cathode with outstanding cyclability for K-ion batteries

Jungmin Kang‡[a], Hyunyoung Park‡[a], Wonseok Ko[a], Yongseok Lee[a], Jinho Ahn[a], Jung-Keun Yoo[b], Seok Hyun Song[c], Hyungsub Kim[c] and Jongsoon Kim*[a]*

[a]Department of Energy Science, Sungkyunkwan University, Suwon, 440-746, Republic of Korea

[b]Carbon Composites Department, Composites Research Division, Korea Institute of Materials Science (KIMS), 797 Changwondaero, Changwon, Republic of Korea

[c]Korea Atomic Energy Research Institute (KAERI), Daedeok-daero 989 Beon-Gil, Yuseong-gu, Daejeon, 34057, Republic of Korea

‡ *These authors contributed equally to this work.*

Corresponding Authors: Dr. Hyungsub Kim (hyungsubkim@kaeri.re.kr), Prof. Jongsoon Kim (jongsoonkim@skku.edu).

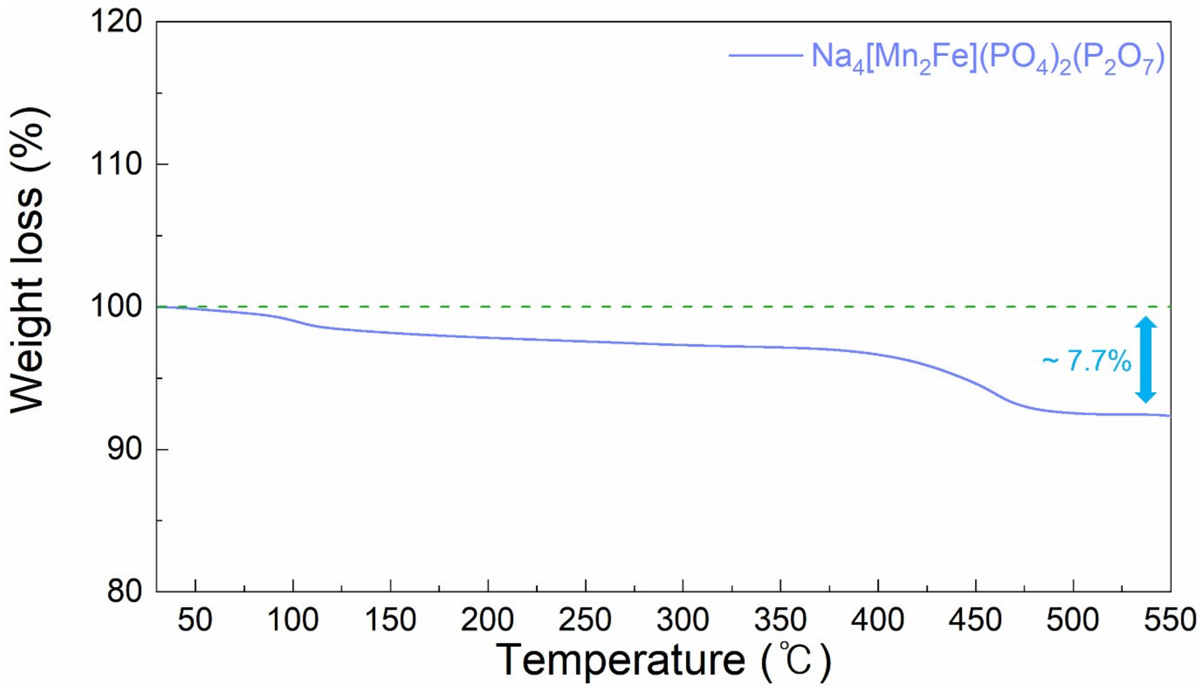

Fig. S1. TGA analysis of pristine $Na_4[Mn_2Fe](PO_4)_2(P_2O_7)$ composite between 30°C and 550°C.

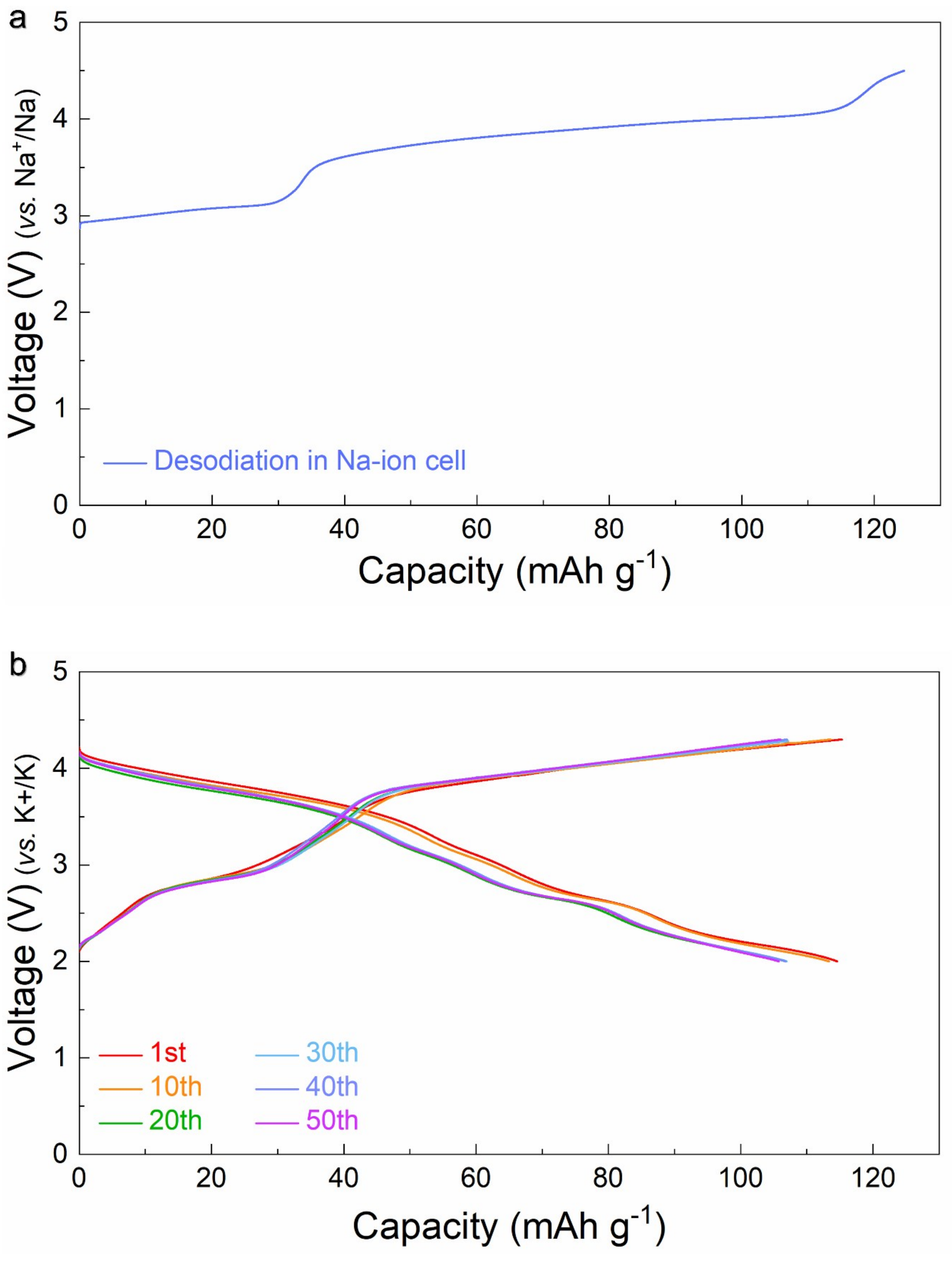

Fig. S2. (a) Electrochemical profiles of $Na_4[Mn_2Fe](PO_4)_2(P_2O_7)$ during desodiation process. (b) Electrochemical profiles of $K_4[Mn_2Fe](PO_4)_2(P_2O_7)$ during Na^+/K^+ ion-exchange process for 50 cycles.

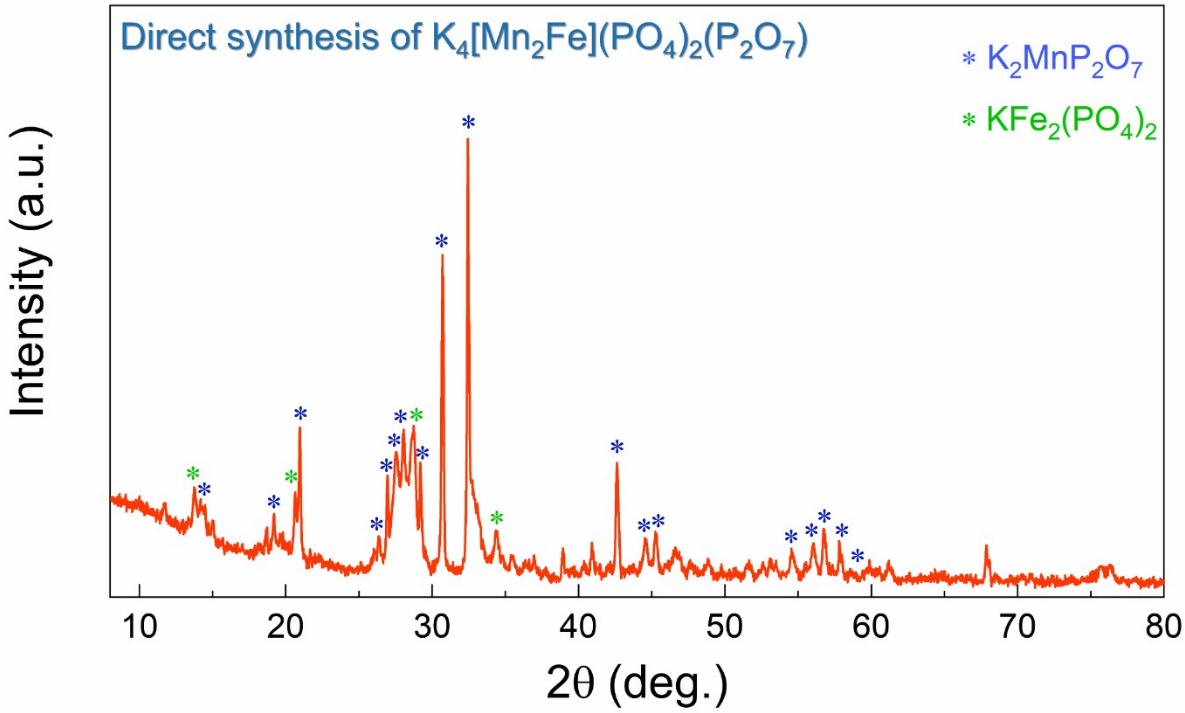

Fig. S3. XRD pattern of sample obtained by direct synthesis of $K_4[Mn_2Fe](PO_4)_2(P_2O_7)$. $K_4P_2O_7$ (97%, Sigma Aldrich), $MnC_2O_4{\cdot}2H_2O$ (Alfa Aesar, 93%), $FeC_2O_4{\cdot}2H_2O$ (99%, Sigma Aldrich), and $NH_4H_2PO_4$ (Daejung, 98%) in a molar ratio of 1:2:1:2 were used as precursors, and 5 wt% pyromellitic acid (PA, $C_6H_{10}O_2$) (Alfa Aesar, 96%) was additionally prepared. The precursors were mixed by high-energy ball milling for 12 h and sealed in an Ar-filled glove box. The mixed powder was calcined at 300°C under Ar flow to remove the organic residues. After calcination, the 5 wt% PA was added and mixed, and the powder was pelletized. The pelletized sample was sintered at 550°C for 12 h under Ar flow.

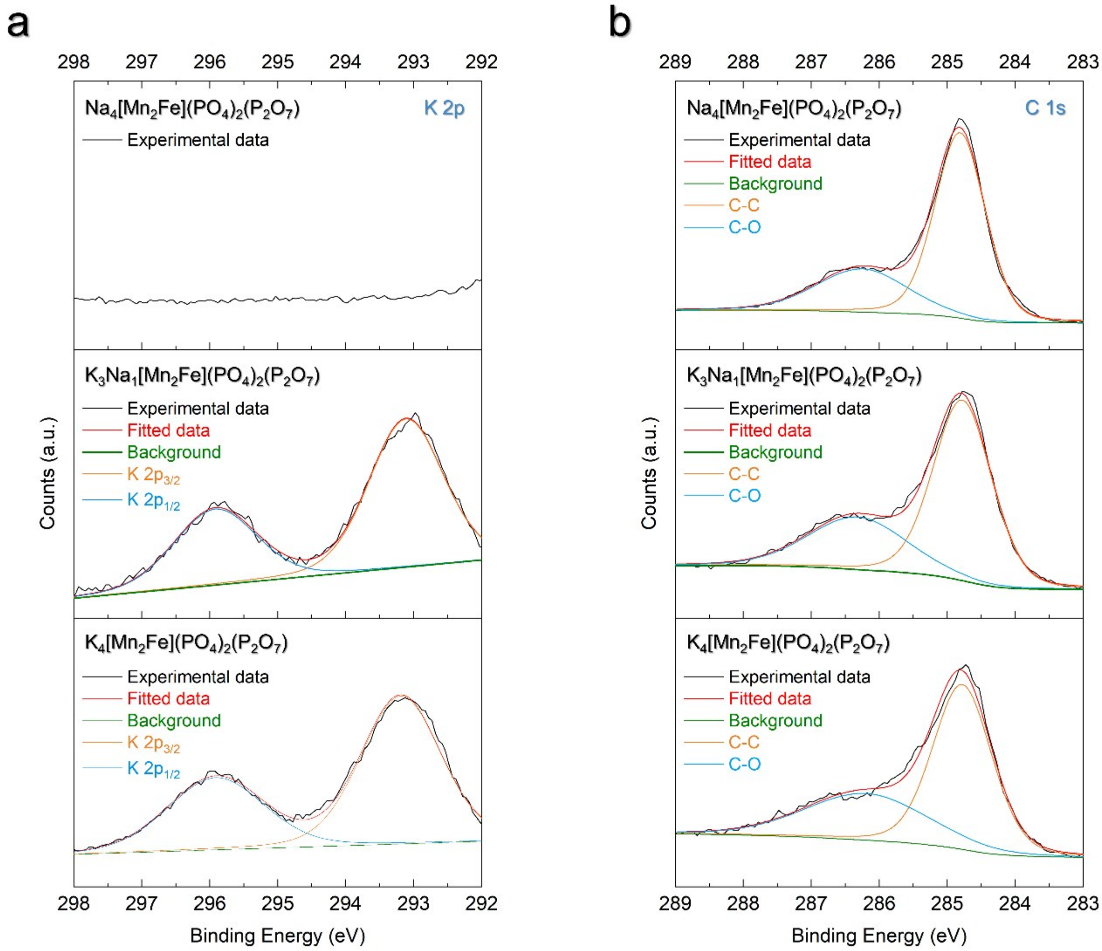

Fig. S4. XPS spectra of $Na_4[Mn_2Fe](PO_4)_2(P_2O_7)$, $K_3Na_1[Mn_2Fe](PO_4)_2(P_2O_7)$ and $K_4[Mn_2Fe](PO_4)_2(P_2O_7)$ during ion-exchange process: (a) K 2p ($2p_{1/2}$: 293.1 eV and K $2p_{3/2}$: 295.9 eV) and (b) C 1s peaks (C-C: 284.78 eV and C-O: 286.2 eV).[1,2]

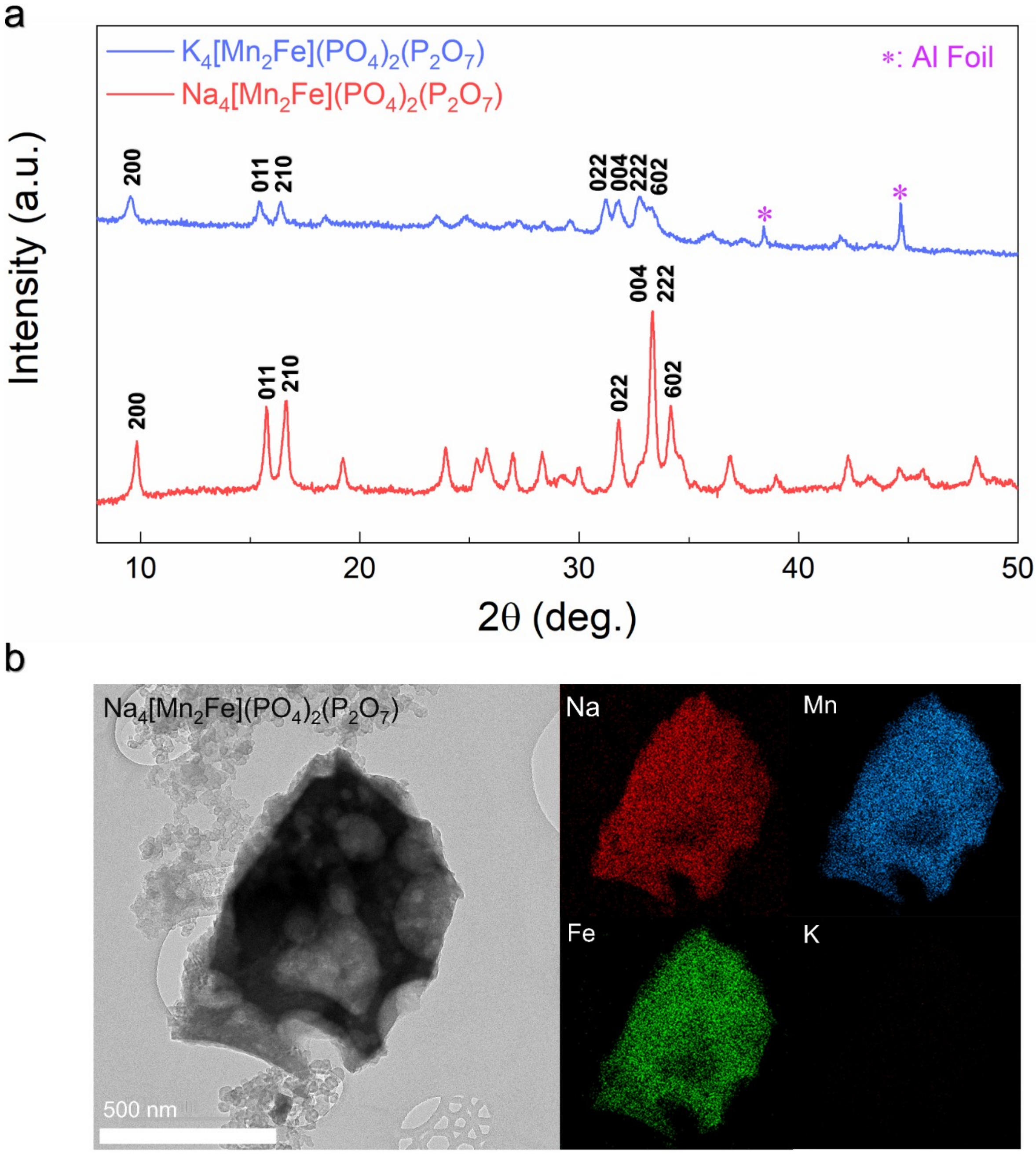

Fig. S5. Characterization of $Na_4[Mn_2Fe](PO_4)_2(P_2O_7)$ and $K_4[Mn_2Fe](PO_4)_2(P_2O_7)$: (a) XRD patterns in the range of 8°–50° and (b) TEM and corresponding EDS mapping of Na, Mn, Fe, and K elements.

a

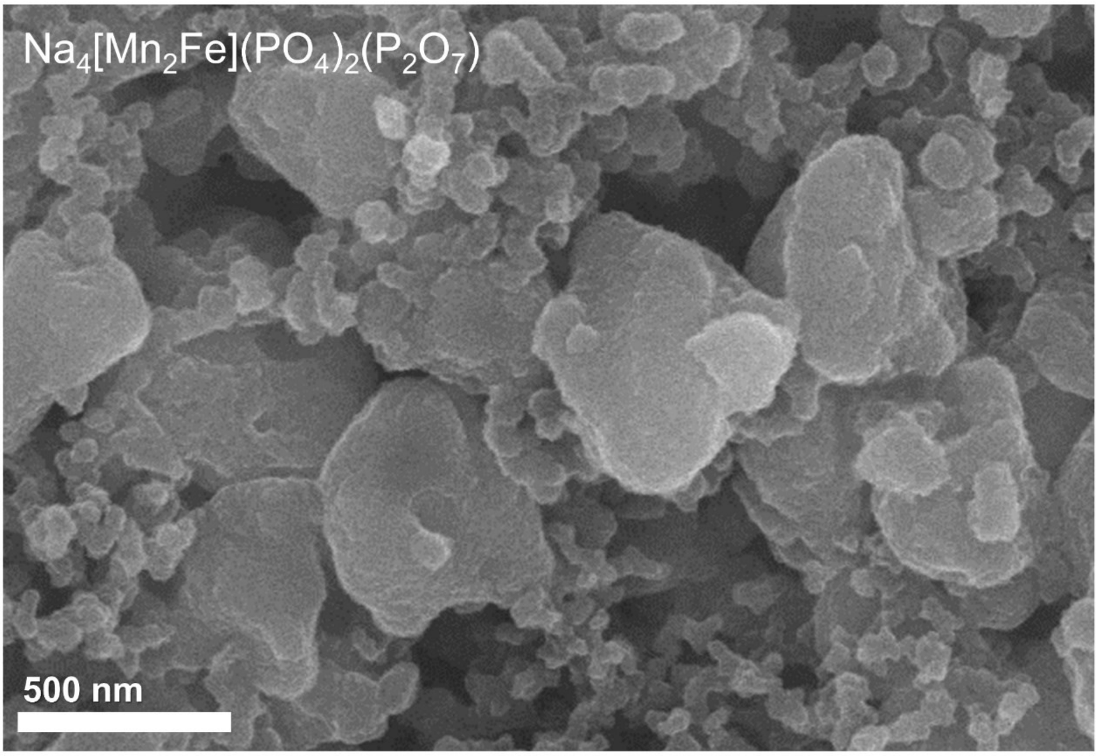

b

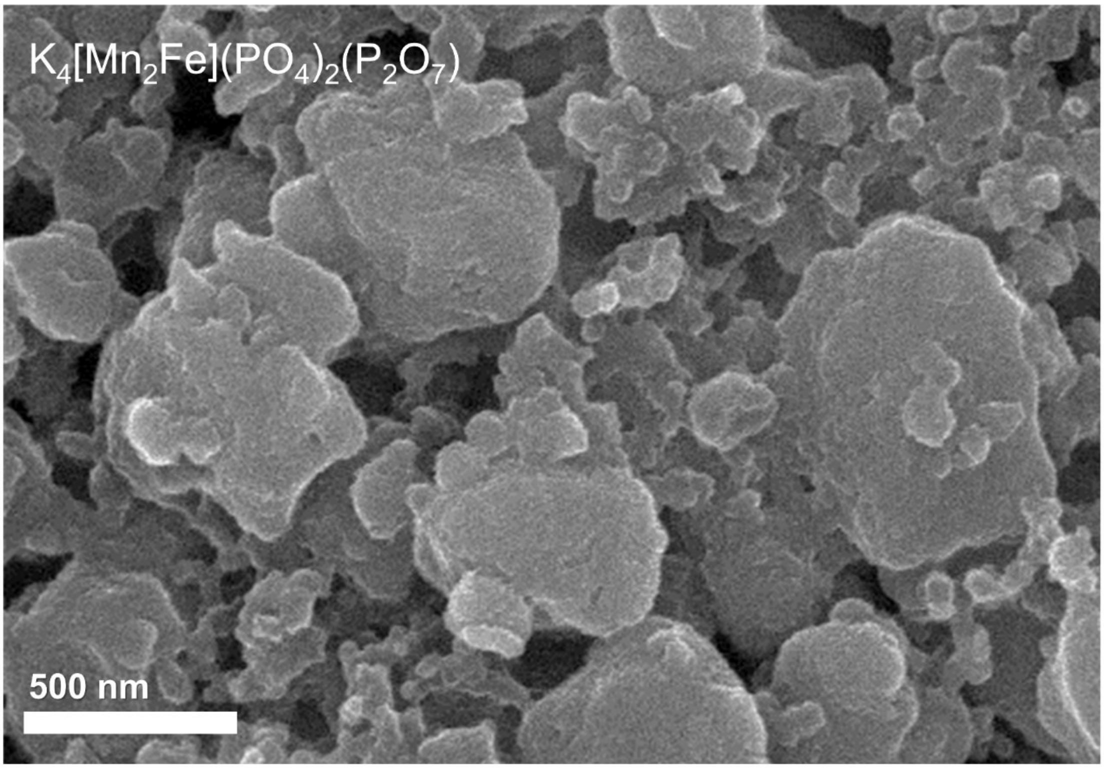

Fig. S6. SEM images of (a) $Na_4[Mn_2Fe](PO_4)_2(P_2O_7)$ and (b) $K_4[Mn_2Fe](PO_4)_2(P_2O_7)$.

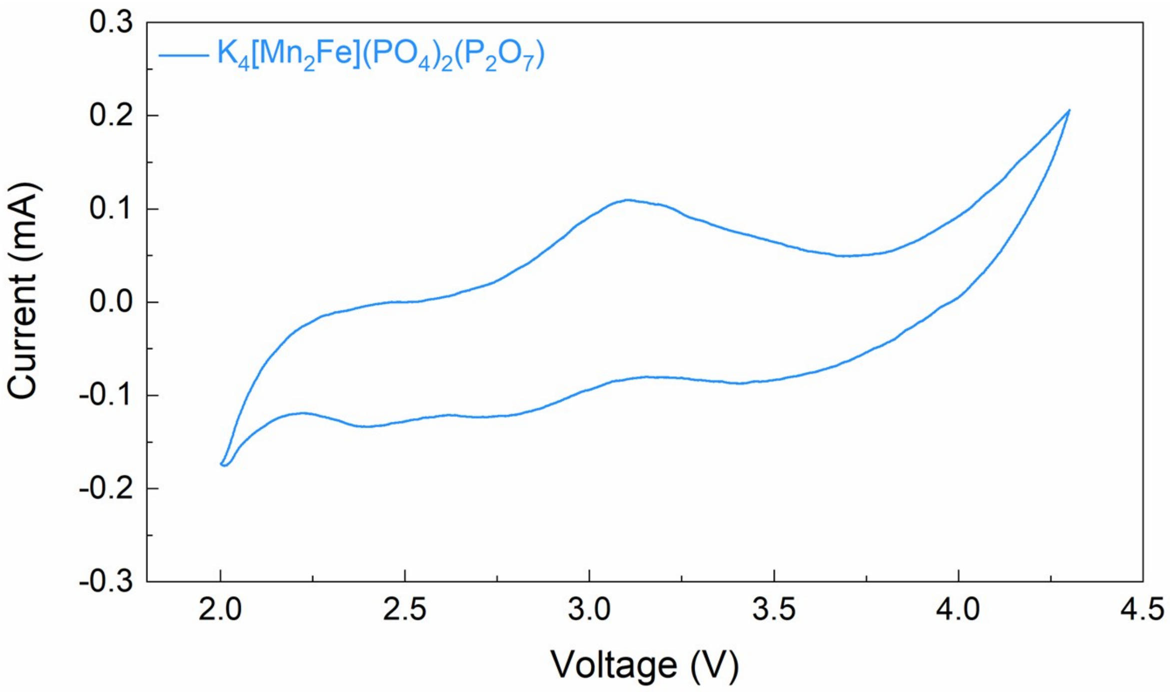

Fig. S7. CV profiles of $K_4[Mn_2Fe](PO_4)_2(P_2O_7)$ with a scan rate of at 1 mV s^{-1} at the voltage range of 2.0-4.3V (*vs.* K^+/K).

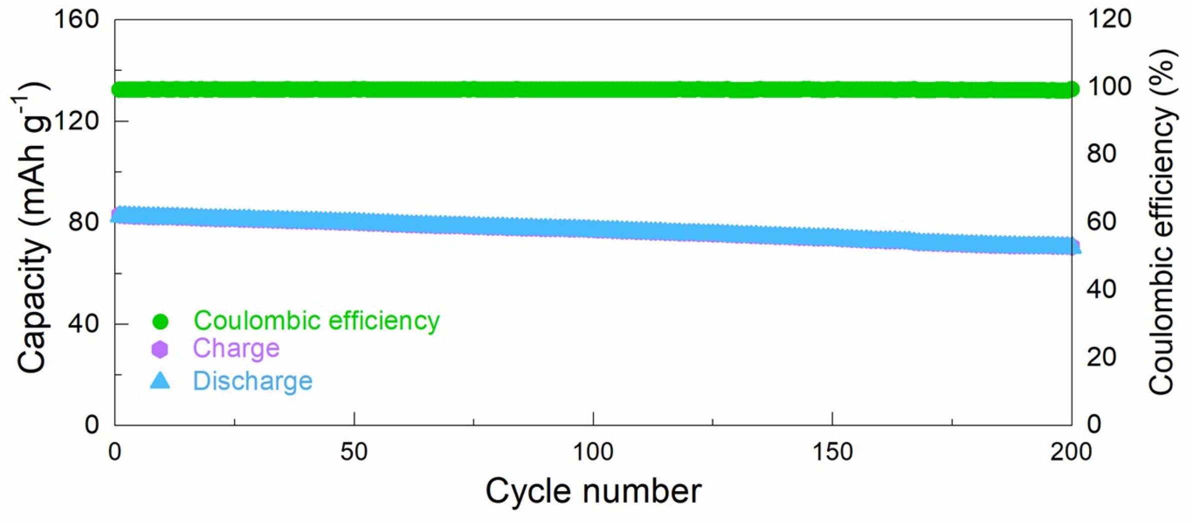

Fig. S8. Cycle performance of $K_4[Mn_2Fe](PO_4)_2(P_2O_7)$ at a high current rate of 5C for 200 cycles in the voltage range of 2.0–4.3 V (*vs.* K^+/K).

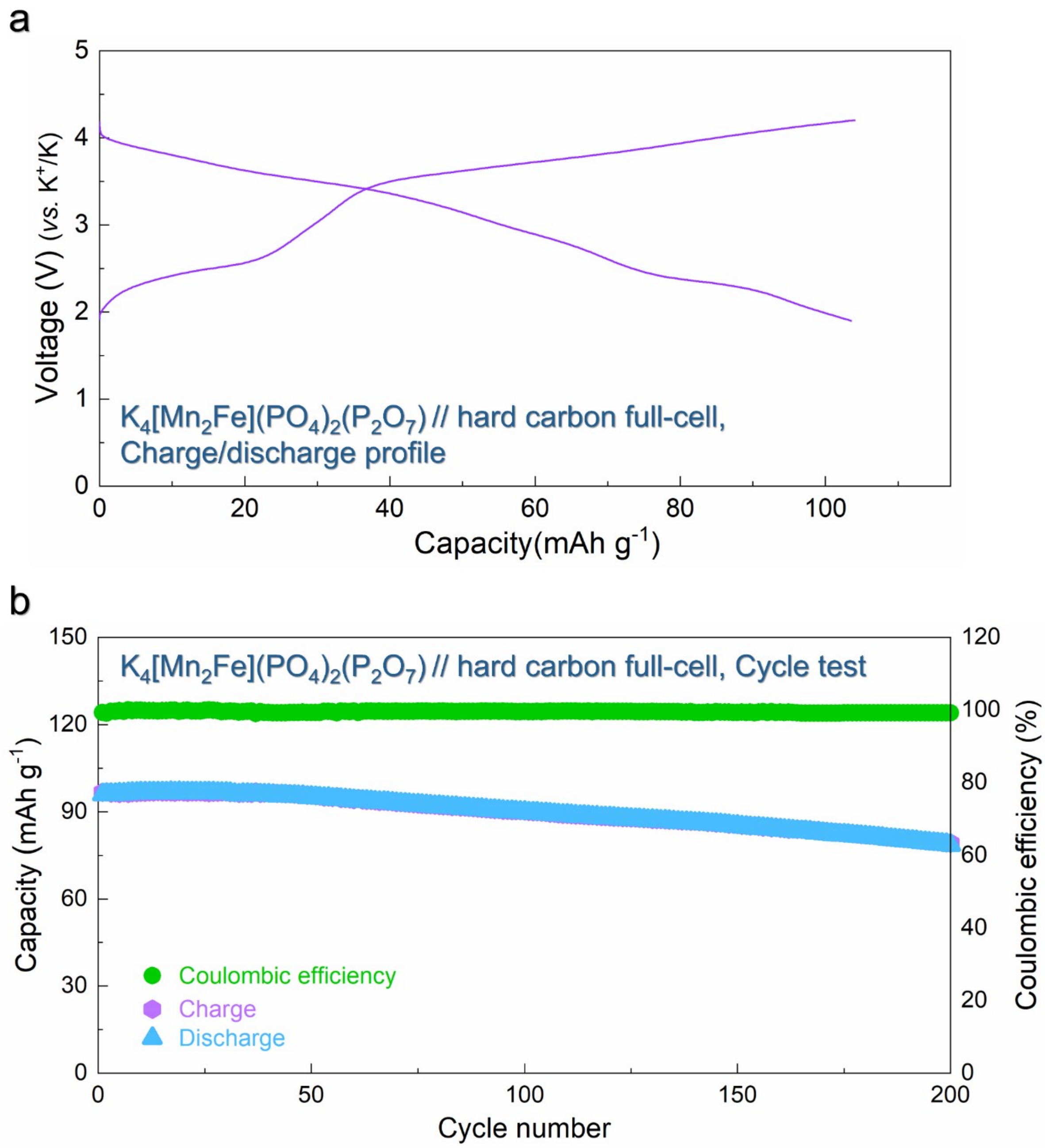

Fig. S9. (a) Initial charge/discharge profile of $K_4[Mn_2Fe](PO_4)_2(P_2O_7)$//potassiated hard-carbon full cell in the range of 1.9–4.2 V at C/20. (b) Cycling performance of $K_4[Mn_2Fe](PO_4)_2(P_2O_7)$//potassiated hard-carbon full cell at C/5 over 200 cycles.

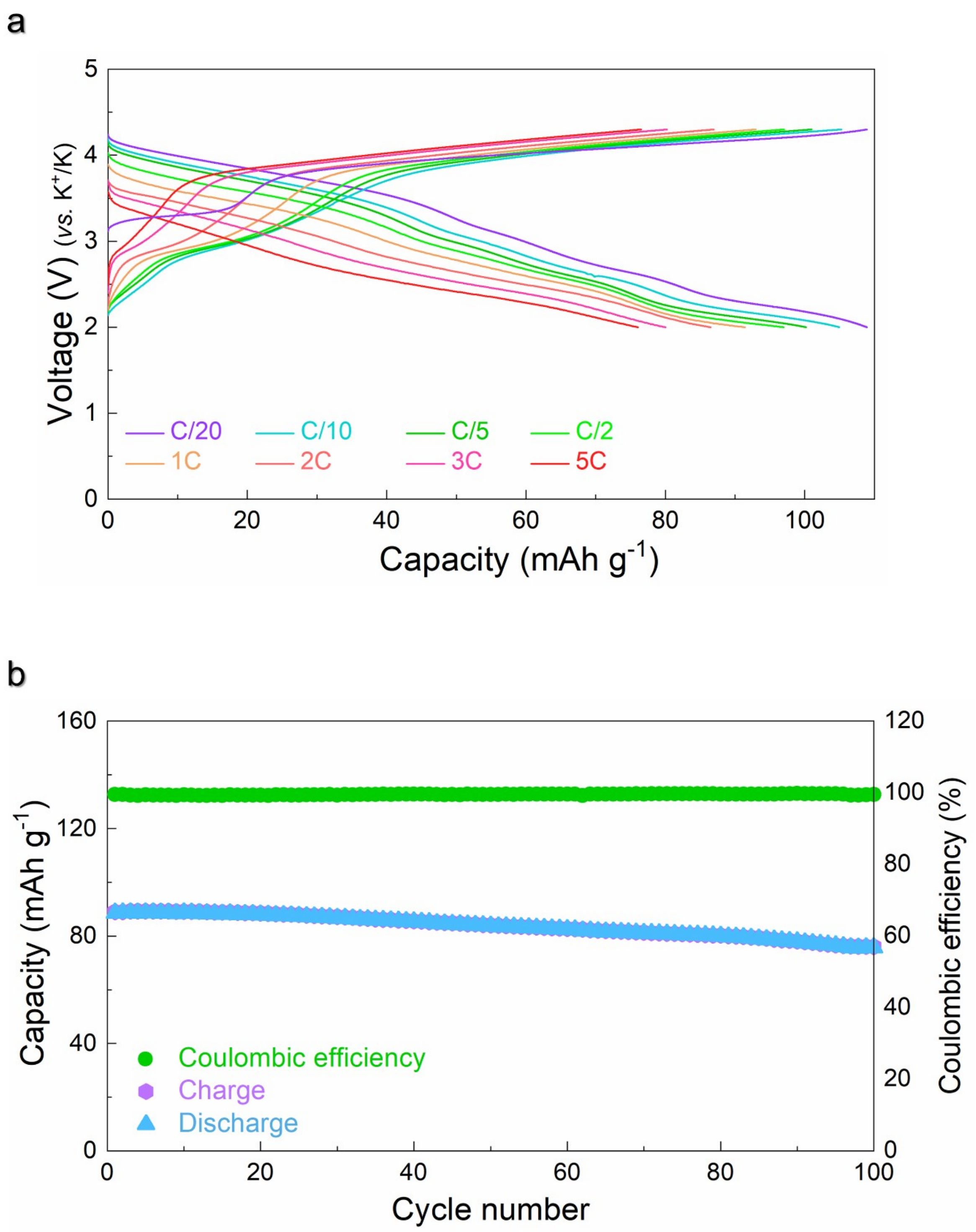

Fig. S10. (a) Power-capability and (b) cycle performance of $Na_4[Mn_2Fe](PO_4)_2(P_2O_7)$ in the voltage range of 2.0–4.3 V (*vs.* K^+/K) under the KIB system.

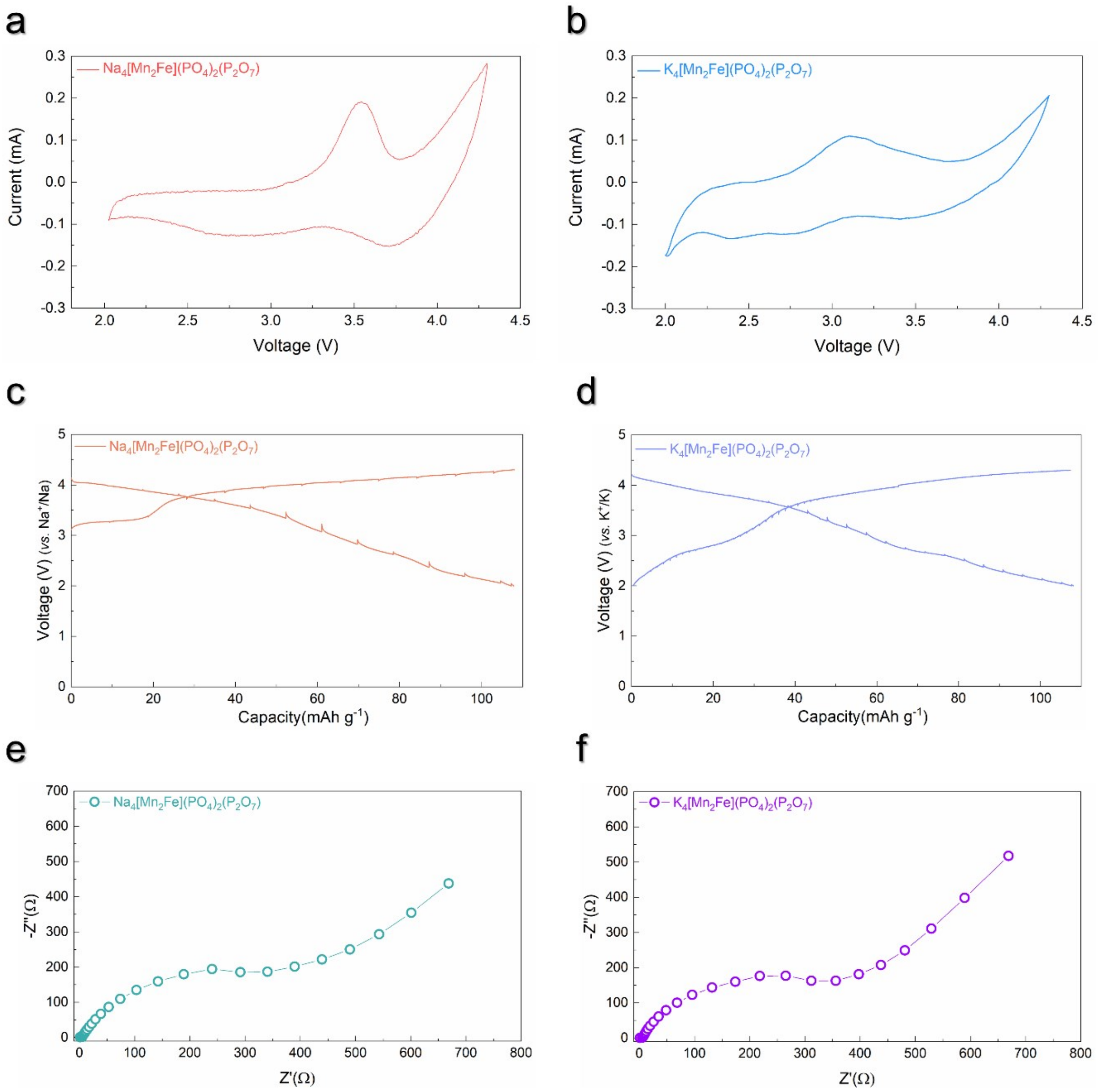

Fig. S11. CV profiles of the (a) $Na_4[Mn_2Fe](PO_4)_2(P_2O_7)$ and (b) $K_4[Mn_2Fe](PO_4)_2(P_2O_7)$ electrode measured at scan rate of 1 mV s^{-1}. GITT profiles of (c) $Na_4Mn_2Fe(PO_4)_2(P_2O_7)$ and (d) $K_4[Mn_2Fe](PO_4)_2(P_2O_7)$ at a current rate of C/10 (1C = 117 mA g^{-1}). EIS profiles of (e) $Na_4[Mn_2Fe](PO_4)_2(P_2O_7)$ and (f) $K_4[Mn_2Fe](PO_4)_2(P_2O_7)$. The experiments above were performed under the KIB system.

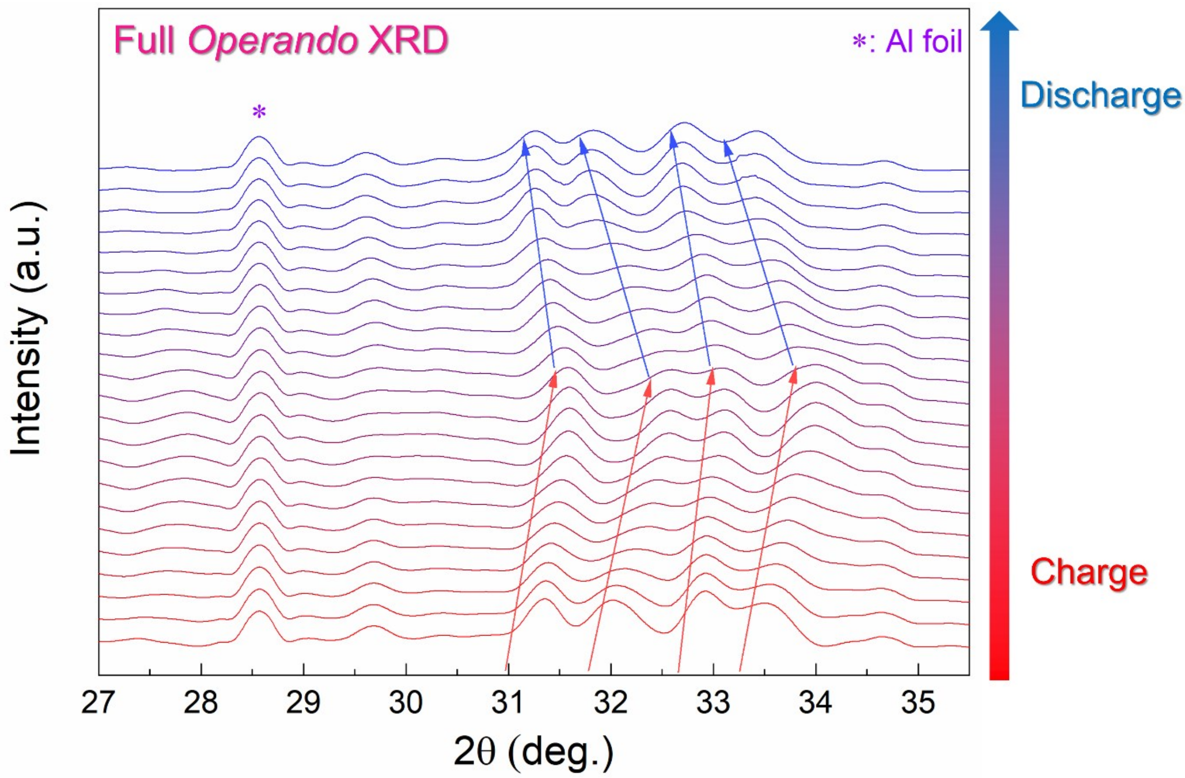

Fig. S12. Full *operando* XRD patterns of $K_x[Mn_2Fe](PO_4)_2(P_2O_7)$ ($1.2 \leq x \leq 4.0$) between 27° and 35.5°.

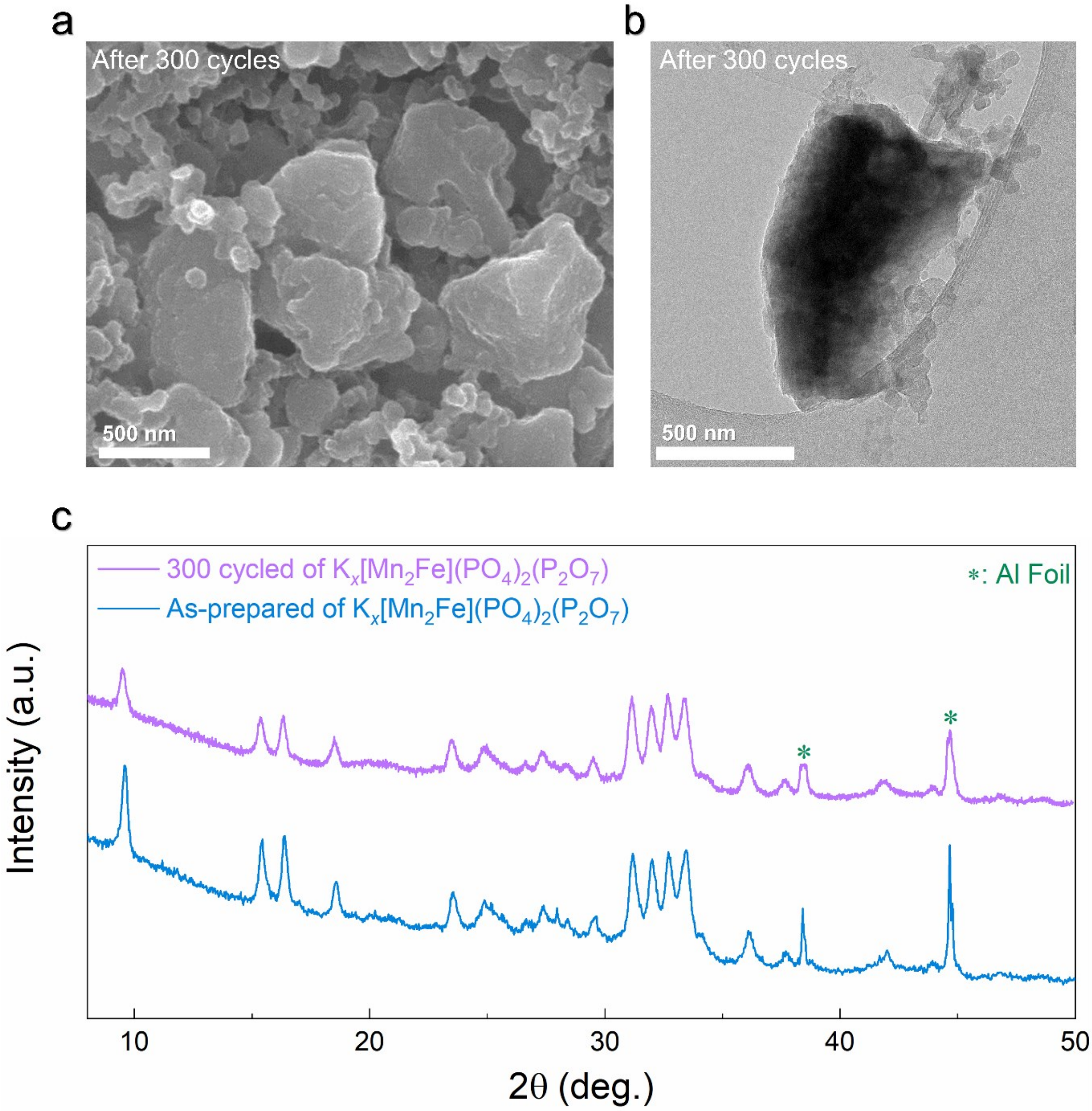

Fig. S13. (a) SEM image, (b) TEM image, and (c) XRD patterns of $K_x[Mn_2Fe](PO_4)_2(P_2O_7)$ ($1.2 \leq x \leq 4.0$) electrode after cycling for 300 cycles in the range of 8°–50°.

	Na	Mn	Fe	K
$Na_4[Mn_2Fe](PO_4)_2(P_2O_7)$	3.997	2.004	1.000	0
$K_3Na_1[Mn_2Fe](PO_4)_2(P_2O_7)$	1.004	2.003	1.000	2.992
$K_4[Mn_2Fe](PO_4)_2(P_2O_7)$	0	2.001	1.000	3.997

Table S1. ICP analyses on the atomic ratio of Na, Mn, Fe, and K of various $K_xNa_{4-x}[Mn_2Fe](PO_4)_2(P_2O_7)$ phases formed during the ion-exchange process from $Na_4[Mn_2Fe](PO_4)_2(P_2O_7)$ to $K_4[Mn_2Fe](PO_4)_2(P_2O_7)$.

Sample	*a*	*b*	*c*	Volume
$Na_4[Mn_2Fe](PO_4)_2(P_2O_7)$	17.9526(4)	6.6018(2)	10.7312(4)	1271.87(5)
$K_4[Mn_2Fe](PO_4)_2(P_2O_7)$	18.2501(7)	6.6450(2)	11.1393(4)	1350.89(9)

Table S2. Comparison of lattice parameters and volume of $Na_4[Mn_2Fe](PO_4)_2(P_2O_7)$ and $K_4[Mn_2Fe](PO_4)_2(P_2O_7)$.

Atom	Wyckoff Position	*x*	*y*	z	B_{iso}	Occupancy
K1	4a	0.5000(13)	0.751(2)	0.9780(16)	0.95(9)	0.83328
K2	4a	0.2891(8)	0.8530(18)	0.7792(17)	0.95(9)	1.00000
K3	4a	0.3940(7)	0.4219(16)	0.259(3)	0.95(14)	0.98185
K4	4a	0.4875(10)	0.714(2)	0.5481(16)	0.95(18)	0.80000
Fe1	4a	0.3398(4)	0.091(3)	0.5018(12)	1.20(6)	0.33330
Fe2	4a	0.1367(4)	0.594(4)	0.4862(12)	1.20(6)	0.33330
Fe3	4a	0.2415(6)	0.316(2)	0.753(2)	1.20(6)	0.33330
Mn1	4a	0.3398(4)	0.091(3)	0.5018(12)	1.20(6)	0.66670
Mn2	4a	0.1367(4)	0.594(4)	0.4862(12)	1.20(6)	0.66670
Mn3	4a	0.2415(6)	0.316(2)	0.753(2)	1.20(6)	0.66670
O1	4a	0.2440(19)	0.568(9)	0.596(3)	0.99(14)	1.00000
O2	4a	0.3560(17)	0.431(5)	0.487(4)	0.99(14)	1.00000
O3	4a	0.3500(17)	0.768(5)	0.533(3)	0.99(14)	1.00000
O4	4a	0.2508(19)	0.592(8)	0.393(3)	0.99(14)	1.00000
O5	4a	0.2307(18)	0.099(9)	0.607(3)	0.99(14)	1.00000
O6	4a	0.1239(16)	-0.110(5)	0.498(3)	0.99(14)	1.00000
O7	4a	0.2369(19)	0.042(7)	0.378(3)	0.99(14)	1.00000
O8	4a	0.1314(15)	0.263(5)	0.453(3)	0.99(14)	1.00000
O9	4a	0.4833(19)	0.359(6)	0.706(3)	0.99(14)	1.00000
O10	4a	0.5486(20)	0.551(7)	0.853(3)	0.99(14)	1.00000
O11	4a	0.6241(14)	0.296(4)	0.739(6)	0.99(14)	1.00000
O12	4a	0.5775(19)	0.601(8)	0.643(3)	0.99(14)	1.00000
O13	4a	0.4658(19)	0.095(8)	0.864(3)	0.99(14)	1.00000
O14	4a	0.3676(15)	0.175(5)	0.713(3)	0.99(14)	1.00000
O15	4a	0.480(2)	-0.007(6)	0.624(3)	0.99(14)	1.00000
P1	4a	0.3016(8)	0.584(5)	0.502(2)	0.57(10)	1.00000
P2	4a	0.1774(8)	0.085(6)	0.490(2)	0.57(10)	1.00000
P3	4a	0.5596(7)	0.4579(17)	0.743(4)	0.57(10)	1.00000
P4	4a	0.4448(8)	0.156(2)	0.749(3)	0.57(10)	1.00000

Table S3. Detailed structural information for $K_4[Mn_2Fe](PO_4)_2(P_2O_7)$ obtained through Rietveld refinement.

Active Materials	Electrolyte	Voltage Range (V)	Specific Capacity (mAh g^{-1})	Cycle Retention (%)	Experimental condition	Ref.
$K_4[Mn_2Fe](PO_4)_2(P_2O_7)$	0.5 M KPF_6 in EC:DEC (1:1 v/v%)	2.0-4.3	110.0	83.0	300 cycles at 39.0 mA g^{-1}	This work
$K_{0.45}MnO_2$	0.8 M KPF_6in EC:DEC (1:1 v/v%)	1.5-4.0	128.6	70.8	100 cycles at 20.0 mA g^{-1}	38
$K_{0.7}Fe_{0.5}Mn_{0.5}O_2$	0.8 M KPF_6 in EC:DMC (1:1 v/v%)	1.5-4.0	178.0	89.0	60 cycles at 100.0 mA g^{-1}	39
P2-$K_{2/3}[Ni_{1/3}Mn_{2/3}]O_2$	0.5 M KPF_6 in EC:DEC (1:1 v/v%)	1.5-4.5	82.0	96.8	200 cycles at 86.0 mA g^{-1}	40
P3-$K_{0.54}[Co_{0.5}Mn_{0.5}]O_2$	1.0 M $NaClO_4$ in EC:PC (1:1 v/v%)	1.5-3.9	120.4	85.0	100 cycles at 20.0 mA g^{-1}	41
$K_{0.5}V_2O_5$	1.5 M KFSI in EC:DEC (1:1 v/v%)	1.5-3.8	90.0	81.0	250 cycles at 100.0 mA g^{-1}	42
$K_3V_2(PO_4)_3$/C	0.8 M KPF_6 in EC:DEC (1:1 v/v%)	2.5-4.3	54.0	81.4	100 cycles at 20.0 mA g^{-1}	43
$K_3V_2(PO_4)_2F_3$	1.0 M KPF_6 in EC:PC (1:1 v/v%)	2.0-4.6	100.0	95.0	180 cycles at 90 mA g^{-1}	44
KVP_2O_7	0.5 M KPF_6 in EC:DEC (1:1 v/v%)	2.0-5.0	60.0	84.9	100 cycles at 25.0 mA g^{-1}	45

Table S4. Electrochemical properties of various cathode materials for KIBs.

Reference

1 R. Sawyer, H. W. Nesbitt and R. A. Secco, *J. Non. Cryst. Solids*, 2012, **358**, 290–302.

2 L. Liu, S. Wang, Z. Zhang, J. Fan, W. Qi and S. Chen, *Ionics (Kiel).*, 2019, **25**, 1035–1043.